Preferential Flow in Water-Repellent Sands

Tim W. J. Bauters, David A. DiCarlo, Tammo S. Steenhuis,* and Jean-Yves Parlange

ABSTRACT

Water-repellent soils occur all over the world and affect both groundwater pollution and crop yield. The finger-like wetting patterns in these soils have many similarities with unstable wetting fronts in coarse-grained sandy soils. Our objectives were to study the water movement in water-repellent sand and to examine how the theory for unstable wetting fronts applies to water-repellent sands. Infiltration experiments, in which moisture content and matric potentials were measured, were carried out in slab chambers with identical sands but with different levels of water repellence. Soil water characteristics were determined in separate experiments. Infiltration in the hydrophilic soil resulted in a uniform and horizontal front. All water-repellent sands showed a fingered flow pattern. For negative water-entry values, water infiltrated without delay. For positive values, water entered the soil only after the depth of the ponded water equaled or exceeded the water-entry pressure, which increased with increasing repellency. The finger widths predicted with the unstable flow theory agreed rather well with the observed values. In general, the research showed that the wetting patterns of water-repellent sands depended directly on the soil water characteristic curve. This implies that the type of wetting front and risk to groundwater pollution can be predicted based on laboratory-measured soil hydraulic properties.

Soils that have hydrophobic properties (also called *water-repellent soils*) can resist or retard surface water infiltration (Brandt, 1969). This affects plant growth and surface water distribution. These soils can be found, for instance, in Florida, Arizona, and California (DeBano, 1969), as well as abroad, in New Zealand, England, Australia (Bond, 1969), and the Netherlands (Hendrickx et al., 1988; Dekker and Ritsema, 1994). Water-repellent soils may be more prevalent than is commonly acknowledged (Bond, 1964; Gilmour, 1968; DeBano, 1969; Marshall and Holmes, 1979; Nakaya, 1982; Dekker and Ritsema, 1996). Some researchers suggest that repellency is the norm rather than the exception (Dekker, 1988; Dekker and Jungerius, 1990; Wallis and Horne, 1992).

Besides the retardation or resistance of surface water infiltration, water-repellent soils have been associated with preferential flow (Jamison, 1945; Bond, 1964; Gilmour, 1968). Preferential flow paths create spatial variability in soil moisture affecting plant growth (Dekker and Ritsema, 1994). In addition, preferential flow allows much faster transport of water and solutes, therefore creating greater risk of groundwater contamination.

Our objectives were to study the infiltration and moisture content patterns in identical sands with different degrees of water repellency and to relate these patterns to soil hydraulic properties.

T.W.J. Bauters, T.S. Steenhuis, and J.-Y. Parlange, Dep. of Agricultural and Biological Engineering, Cornell Univ., Ithaca, NY 14853; and D.A. DiCarlo, Dep. of Petroleum Engineering, Stanford Univ., Stanford, CA 94305. Received 10 Oct. 1997. *Corresponding author (tss1@cornell.edu).

Published in Soil Sci. Soc. Am. J. 62:1185–1190 (1998).

UNSTABLE FLOW

The stability of the wetting front for different repellencies can be understood heuristically as follows. For gravity-driven displacements, the front is unstable whenever the flux, q, is less than the soil's unsaturated conductivity, $K(\theta)$ (Saffman and Taylor, 1958):

$$q < K(\theta) \qquad [1]$$

When the wetting pressure–saturation curve has little or no slope (the repellent sands), the wetting front is very abrupt, and directly behind it the saturation is very high. This leads to a high conductivity and the instability criterion is satisfied. When the wetting pressure–saturation curve has an appreciable slope (the nonrepellent sand), the wetting front is not as abrupt. Thus, we observe a situation where the sand wets only to a saturation such that the conductivity equals the flux, and the instability criterion is not satisfied.

The equation for finger diameter was originally proposed by Parlange and Hill (1976), and can be simplified with the method in Liu et al. (1994) to

$$d \approx \frac{2\pi\theta_f \dfrac{dh}{d\theta}}{(\eta + 1.5)\left(1 - \dfrac{v_f\theta_f}{K_f}\right)} \qquad [2]$$

where:

- d = finger width, cm
- θ_f = moisture content at finger tip, $cm^3\ cm^{-3}$
- η = exponent in the Brooks and Corey (1964) conductivity equation; for sand, the exponent varies between 3.3 and 3.7 (Liu et al., 1994)
- v_f = velocity of finger, $cm\ s^{-1}$
- K_f = conductivity near wetting front, $cm\ s^{-1}$

The original equation of Liu et al. (1994) assumed that the velocity was very much smaller than the saturated conductivity and did not include the velocity term in the denominator. As we will see below, this assumption is not met for most of the water-repellent soils where the ponded water flows rapidly through the soil.

MATERIALS AND METHODS

Blasting silica sand (W.F. Saunders & Sons, Etna, NY[1]) was used as the substrate to analyze the effect of repellency. Table 1 shows the textural composition. Different degrees of water repellency were added to the sand through the following procedure. An ethanol solution containing 4.8% octadecyltrichlorasilane (OTS) was mixed in a cement mixer for 5 h with 25 kg of blasting sand, which produced an extremely water-

[1] Mention of product names does not suggest an endorsement of the product.

Abbreviations: OTS, octadecyltrichlorasilane; WDPT, water drop penetration time.

Table 1. The screen analysis (by weight) of the blasting silica sand provided by manufacturer, W.F. Saunders & Sons.

Screen opening	Accumulated sand

repellent sand after drying (Bradford and Leij, 1996). A basis sand batch was made by mixing 3 kg of the extremely repellent sand with 45 kg of regular nonrepellent sand. This basis sand was then diluted with regular sand to achieve different degrees of repellency (Table 2). The most repellent sand tested was achieved by mixing 1 kg of the undiluted repellent sand with 10 kg of regular sand. In Table 2, the first number in the notation for the batches refers to the amount, in kilograms, used of the basis repellent sand (except for the most repellent sand) and the second number refers to the amount, in kilograms, of the regular sand. The degree of repellency is defined by the amount of highly repellent sand (the sand that was

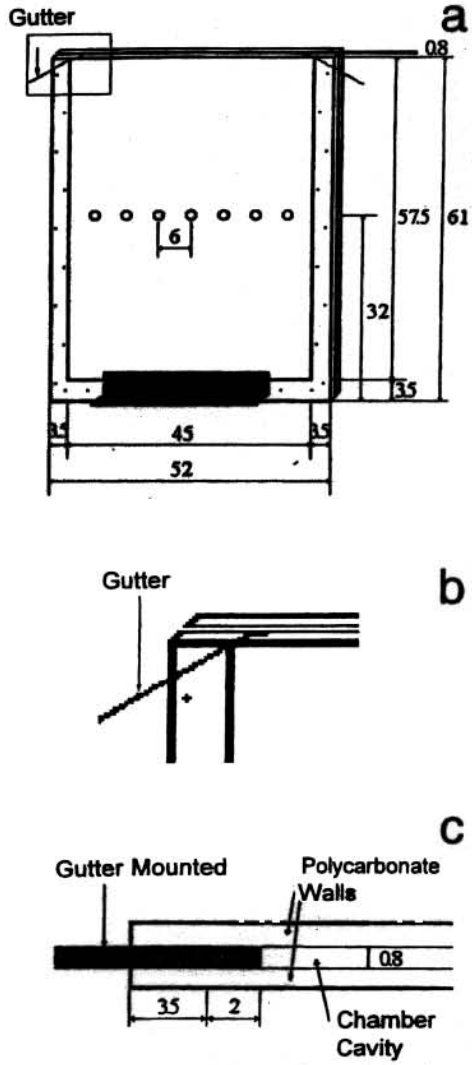

Fig. 1. Schematic diagram of the experimental chamber: (a) front view; (b) detail of the left corner of the chamber with gutter; (c) top view. Dimensions are given in centimeters.

Table 2. The water drop penetration time (WDPT)† for the different batches of water-repellent sand.

Water-repellent ratios		WDPT	
Batch type ‡	Water repellency	WDPT	Description
	%	s	
Regular	0	<0.5	Wettable (<5 s)
10+10	3.13	40	Slightly water repellent (5–60 s)
10+2.5	5.00	2400	Severely water repellent (600–3600 s)
6+0.6	5.68	>3600	Extremely water repellent
1+10§	9.01	>3600	Extremely water repellent

† The WDPT test consists of randomly applying a single water drop (0.05 mL) onto the sand surface and measuring the amount of time (in seconds) it takes to infiltrate the soil (Letey, 1969; King, 1981).

‡ The first number in the notation for the batches refers to the amount, in kilograms, used of the basis repellent sand (except for the most repellent sand) and the second number refers to the amount, in kilograms, of the regular sand.

§ The most repellent sand was achieved by mixing 1 kg of the undiluted repellent sand with 10 kg of regular sand.

mixed with OTS in an ethanol solution) vs. the total amount of sand used.

Besides the ratio of repellent to nonrepellent sand, the water drop penetration time (WDPT) was used to quantify the degree of repellency. The WDPT test consists of randomly applying a single water drop (0.05 mL) onto the sand surface and measuring the amount of time (in seconds) it takes to infiltrate the soil (Letey, 1969). Table 2 shows that the soil batches ranged from wettable, via slightly repellent, to severely and extremely water repellent (Letey, 1969; King, 1981).

A polycarbonate slab chamber was built to observe and quantify the preferential flow phenomena (Fig. 1). The interior dimensions of the chamber were 45 cm wide, 57.5 cm tall, and 0.8 cm thick with 1-cm polycarbonate walls. Seven high-speed tensiometers, to measure water pressures, were threaded into the chamber at a height of 32 cm and 6-cm horizontal spacing. Each tensiometer consisted of a flat stainless porous plate (0.8-cm diameter, 2-μm pore size) sealed in a hollow brass housing (Selker et al., 1992a). The tensiometers were inserted so the porous plate was flush with the inside of the chamber to minimize their effect on packing and fluid flow. Each tensiometer was filled with degassed water and attached through a stiff nylon tube and a three-way valve to a pressure transducer and a vertical water tube. By turning the valve, the transducer could be connected to the vertical tube for calibration, or to the tensiometer for measurement. The output of the transducers was read by a data acquisition system, consisting of a personal computer with an A-D board and a multiplexer to process a total of 16 incoming channels.

The chamber was filled under a hopper with three randomizing screens (Glass et al., 1989a). Before every filling, an extension of 15 cm was put on top of the chamber to achieve an homogenous packing in the chamber by removing the poorly packed top section.

For infiltrations, the packed chamber was placed in front of the fluorescent light bank and the tensiometers were attached to the data acquisition system. As wet sand transmits more light than dry sand (Glass et al., 1989b), light transmission was used to quantify moisture content. The experiments were recorded by a black and white camera (Panasonic TV camera WV 1850) and a video cassette recorder (Panasonic AG 6720). The recorded experiments were then digitized with a frame grabber and analyzed with Global Labs Imaging software (Data Translation, Marlborough, MA) to determine the moisture content, the position of the wetting front, and the

finger diameter at regular time intervals. The wetting front position was always associated with the most downward point (i.e., fastest growing finger when the front was unstable). The finger width reported was the average of the widths taken at 5-cm intervals along all fingers just before the water application was stopped.

The water application system consisted of a peristaltic pump-driven point source, which was moved back and forth across the soil surface by a rotating camshaft. To eliminate the fingers flowing along the side edges of the chamber, gutters were installed to prevent rain from falling onto the soil within 2 cm of the chamber side edges (Fig. 1b and 1c). Infiltrations were conducted with an irrigation rate of 0.16 cm min^{-1}. Experiments with infiltration rates between 0.058 and 0.19 cm min^{-1} all produced qualitatively similar results but are not discussed here.

Using the same chamber as was used for the infiltrations, the soil water characteristic curves were determined for all the sands. The drying curves were obtained through the following procedure. A peristaltic pump pumped the water in the bottom of the chamber at a flow rate of 15 cm^3 min^{-1} (equivalent to an increase in water level in the chamber of 0.42 cm min^{-1}). The water was turned off when the water level in the chamber reached a height of 53 cm. The valve was then opened and the water was allowed to drain out of the chamber. After 24 h, the front panel of the chamber was removed and the sand column was segmented in 1-cm levels. Each segment was weighed, dried for 24 h at 105°C, and weighed again. This procedure was practiced on the left and right side of the chamber, which resulted in two drying curves per experiment. Those two were then averaged to obtain the drying curve.

The wetting curves were also determined in the chamber. A constant head was connected to the bottom of the chamber and left connected for 24 h until equilibrium was reached. The chamber was again taken apart to section the sand and to determine the water saturation. The light intensity–moisture content relationship was also obtained as a part of this procedure. Just before the chamber was taken apart, it was placed in front of a fluorescent light bank; the light intensities were recorded and then later related to the moisture contents.

Knowledge of the slope of the primary wetting curve, $dh/d\theta$ is needed for the prediction of the finger diameter. The slopes were determined as follows. For the repellent sand treatments, the slope was determined in the range of 20 to 100% saturation. Since the slopes were within the measurement error for the repellent sands, one average slope was taken.

RESULTS AND DISCUSSION

The soil water characteristic curves are presented first, followed by a description of the patterns of infiltration into the five sands. Finally, the validity of the unstable flow theory for water-repellent sands is discussed. We refer to the different sands by either the water repellency percentage or by the name according to the WDPT test (Table 2).

The mean drying curves for the four repellent sands were the same within the 95% confidence interval (Fig. 2). Only the drying curve for the nonrepellent sand from 50 to 100% saturation was significantly different (i.e., more than two standard deviations away) from the same sand made water repellent. Consequently, the air-entry pressures were also different: −7 cm for the nonrepellent sand and approximately −20 cm for the four water-repellent sands. The slope of the "repellent" primary drying curve at pressures below the air-entry pressure resembled that of a coarser sand. Note that for pressures between 0 and −10 cm, the water-repellent soils have saturation slightly less than 100%, probably because water had difficulty infiltrating in the area between the ports when the chamber was being filled up, which resulted in air inclusions in that area.

Water-entry pressures and the slope of the primary wetting curves were also affected by the water repellency (Fig. 3). The water-entry pressures increased with the degree of repellency (Table 3). For the extremely repellent sands (i.e., 5.68 and 9.01%), the water-entry pressures were positive. The severely water-repellent soil (5.00%) had a value close to zero and the slightly water-repellent sand had a negative water-entry pressure that was half of the nonrepellent sand. In addition, Fig. 3 shows that the slopes of the soil water charac-

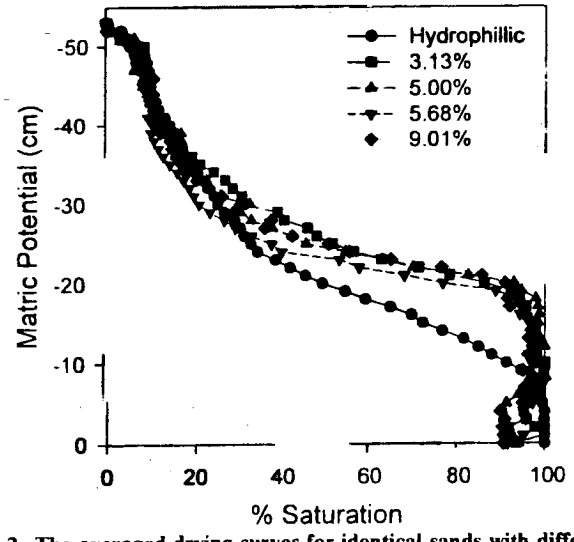

Fig. 2. The averaged drying curves for identical sands with different degrees of repellency. The water-repellent drying curves statistically differ between 50 and 100% saturation from the nonrepellent sand.

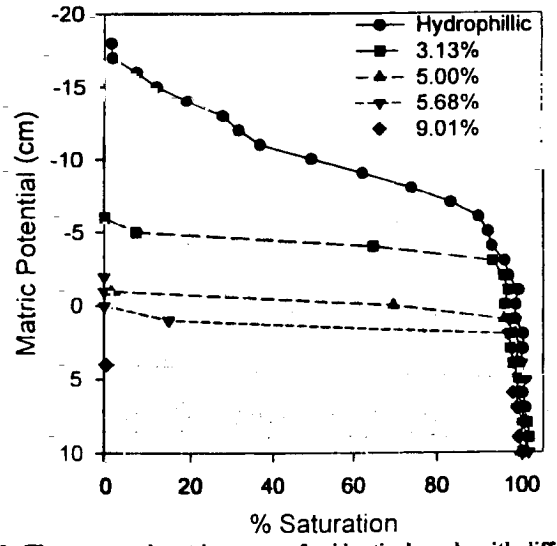

Fig. 3. The averaged wetting curves for identical sands with different degrees of repellency.

Table 3. Water-entry pressures measured with a tensiometer and water-entry values from the wetting curves.

Water repellency	Water-entry pressure data at the fingertip: Data	Water-entry pressure data at the fingertip: Standard deviation	Water-entry pressure data from wetting curves
%	cm		
Regular	−9.3	1.3	−6.0
3.13	−2.2	0.7	−3.0
5.00	−1.5	1.0	−1.0
5.68	3.6	NA†	2.0
9.01	5.6	0.9	5.0

teristic curves for the repellent sands were flatter than for nonrepellent sand.

The infiltration patterns varied significantly for the various sands (Table 4, Fig. 4). For the nonrepellent sand, the water infiltrated as a nearly horizontal uniform front. Although for all the water-repellent sands, fingered-type flow paths developed (Table 4 lists the finger widths), there were differences in time before the water started to infiltrate (Fig. 4). In the slightly repellent sand, there was no time delay. For the remaining repellent sands, ponding occurred before the water infiltrated. The longest ponding was for the most extremely water-repellent sand and lasted until the water depth was approximately equal to the water-entry value. Despite the time required for ponding, the wetting fronts of all the water-repellent sands reached the bottom of the chamber before the uniform wetting front of the nonrepellent sand (Fig. 4), with the severely repellent sand having the shortest arrival time. This infiltration behavior is in accordance with field observations of Hendrickx et al. (1993), in which water repellency shortened the travel time to the groundwater and increased the risk of groundwater pollution.

Front width and water pressures helped to gain better insight into the fingering phenomenon. The pressure before the wetting front passed the tensiometers in Fig. 5 and 6 was meaningless as the sand was air dry and there was no connection to the soil water. For the nonrepellent sand, the uniform front reached the tensiometer at 3260 s, and the pressure at the front approached −11.8 cm and remained approximately the same until the water application was stopped at 8730 s (Fig. 5). The constant pressure after front passage implied that

Table 4. Measured finger width, front water content, number of fingers, front velocity, and dh/d0 values.

Water repellency	Measured finger width	Front water content	Fingers	Front velocity	dh/d0 values
%	cm	$cm^3\ cm^{-3}$			
Regular	45	0.14			
3.13	2.1	0.40			
5.00	2.8	0.41			
5.68	2.7	0.38			
9.01	7.1 (3.55)‡	0.38			

† Not available.
‡ The width in parentheses is half of the total width, because at the bottom 10 cm of the chamber the finger split into two.

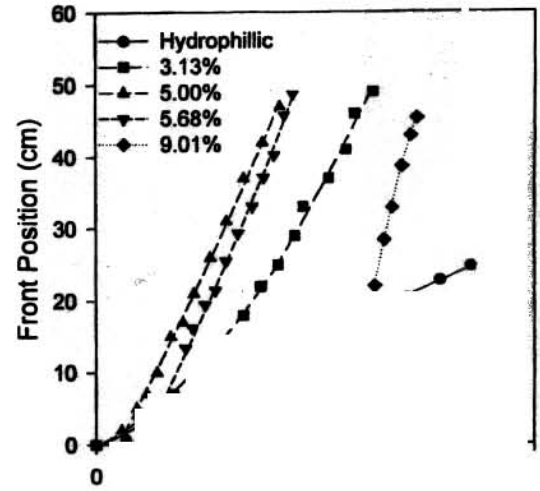

the water at all positions behind the front was driven by a unit gradient, and that the conductivity equaled the downward flux. Thus, as expected for a uniform wetting front, the soil *wets* to the water content such that $K(\theta)$ equals the downward flux. Once the infiltration was stopped, the pressure decreased to −26 cm and gradually went to −30 cm.

As an example of an unstable front, the equivalent time series of the pressure in the 5.68% water-repellent sand (Fig. 6) showed that the front reached the tensiometer at 2200 s. The maximum pressure at the front was 3.6 cm. Immediately behind the front, the pressure quickly decreased to −12 cm. The sharp drop is a typical property of the unstable front (Raats, 1973). In the case of the unstable wetting front, the sand *dries* to the water content such that $K(\theta)$ equals the downward flux (Selker et al., 1992b). Interestingly, the water pressure behind the unstable front was approximately the same as the

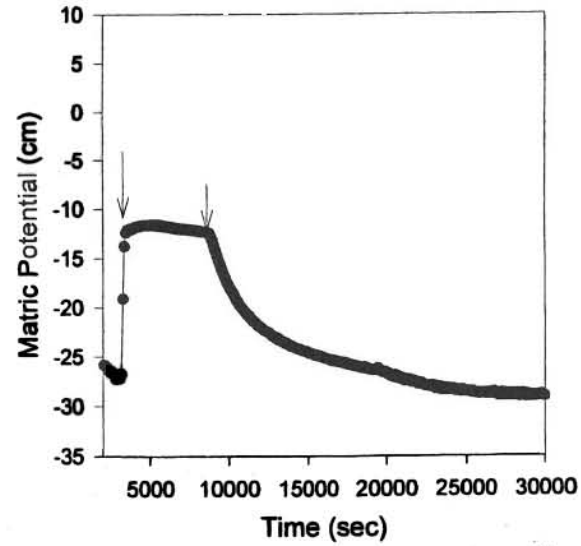

Fig. 5. A time series of the measured tensiometer pressure in regular sand.

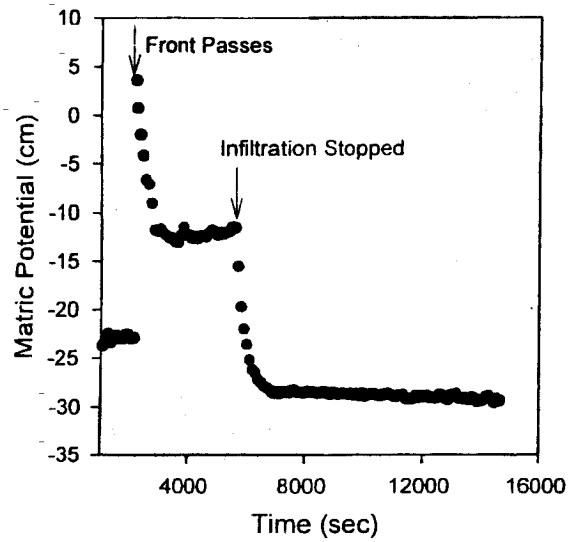

Fig. 6. A time series of the measured tensiometer pressure in 5.6% water-repellent sand.

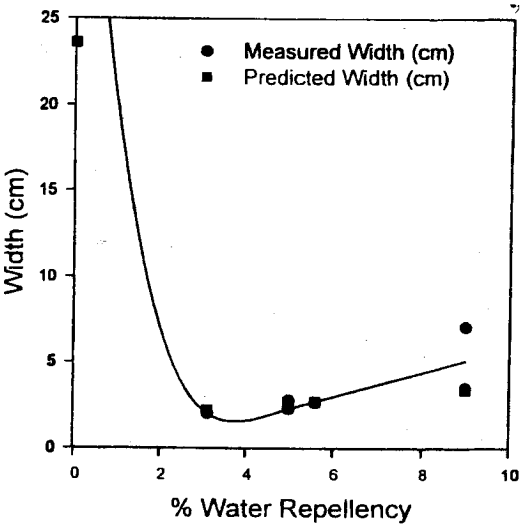

Fig. 8. The measured and predicted finger widths are depicted vs. repellency percentage. The line is a polynomial through the predicted widths.

water pressure behind the stable front, even though there was a higher flux behind the unstable front than behind the uniform front. This is consistent with the primary drying curves in Fig. 2. The soil behind the wetting front was on the drying curve and Fig. 2 shows that at pressures between −7 and −20 cm the nonrepellent soil has, indeed, a lower moisture content than the repellent soil. At the observed pressure behind the front of −12 cm, moisture saturations were 34 and 100% for the nonrepellent and repellent sands, respectively. Because conductivity is uniquely related to the moisture content, the water-repellent sand had a higher conductivity than the nonrepellent sand even though the pressures were the same. Once the infiltration was stopped, the pressure further decreased rapidly to −27 cm and gradually moved to −30 cm. This post-infiltration pressure decrease dropped at a rate that was much higher than in the nonrepellent sand.

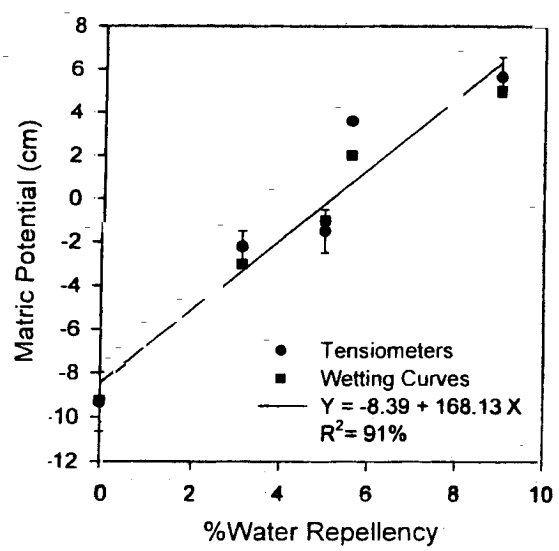

Fig. 7. The water-entry pressure obtained from the wetting pressure–saturation curves and the tensiometer readings directly behind the front vs. repellency percentage. The error bars indicate the standard deviation for the tensiometer measurements. The line is a linear regression on the tensiometer measurements and has a R^2 of 91%.

Examining the water-entry pressure and the maximum water pressure at the wetting front from Table 3 as a function of the repellency percentage of the sand, Fig. 7 shows that the maximum pressure and the water-entry pressure closely matched and both increased linearly with the degree of repellency (R^2 = 91 and 97% for the wetting front pressures and water-entry values, respectively).

Equation [2] predicts that the flatter the primary wetting curve, the smaller the finger. Also, if the ratio of finger velocity and conductivity increases, we expect a wider finger. In the case of a stable wetting front, this ratio becomes equal to one, resulting in an infinite width. For the unstable fingers, the finger tips were saturated and the K_f equaled the saturated conductivity that, in a separate downflow experiment in a tube with a radius of 1 cm, was determined to be 4.7 cm min^{-1}. The η was taken to be 3.3 (Liu et al., 1994).

The measured (Table 4) and predicted finger widths vs. repellency percentage are plotted in Fig. 8 (the standard deviations of the measured widths are smaller than the symbols). Measured finger widths for the repellent sand were approximately 3 cm except for the most extremely repellent (9.01%) sand, for which the width was 7.1 cm or nearly double the width of the other fingers. The predictions match the measured finger widths, in general, very well. Although the finger width for the 9.01% repellent sand was predicted to be larger because of its higher velocity, it did not match the 7.1-cm width. Close examination of the video revealed that the tip of the finger in the bottom 10 cm of the chamber was splitting into two. Thus, possibly, the wide finger could have been two smaller fingers traveling together. The predicted widths for the nonrepellent sand were larger than the chamber width. This is in accordance with the flat wetting front observed in the chamber.

An interesting observation was that the finger–front velocity increases with the degree of repellency of the

sand (Table 4). A simple argument on how repellency enhances the velocity of fingers may be derived from the research of Weitz et al. (1987). They found that the velocity of the fluid–fluid interface (the water front in this case) increases with the pressure drop at the interface. For our case, as the sand was more repellent, a higher water pressure needed to be reached before water could enter it. Hence, the velocities increased as the sand became more water repellent. Finger velocity also affected the number of fingers: the higher the velocity and the lower the flux, the fewer the fingers.

In summary, we have shown that by making identical sands water repellent, unstable water fronts and preferential flow patterns were created where none existed before. Water repellency directly affected the soil water characteristics, and these changes were represented in the preferential flow characteristics. Finger velocity and water-entry pressure were both linearly related to the water repellency of the sand. Finger widths could be predicted with unstable flow theory. This implied, for field soils, that water repellency, or lack thereof, played a controlling role in the creation of preferential flow and groundwater pollution, such as was already shown experimentally by Hendrickx et al. (1993).

REFERENCES

Bond, R.D. 1964. The influence of the microflora on the physical properties of soils. Field studies on water repellent sands. Aust. J. Soil Res. 2:123–131.

Bond, R.D. 1969. The occurrence of water-repellent soils in Australia. p. 1–6. *In* Proc. Symp. Water Rep. Soils, Riverside, CA. 6–10 May 1968. Univ. of Calif., Riverside.

Bradford, S.A., and F.J. Leij. 1996. Predicting two- and three-fluid capillary pressure–saturation relationships of porous media with fractional wettability. Water Resour. Res. 32:251–259.

Brandt, G.H. 1969. Water movement in hydrophobic soils. p. 91–115. *In* Proc. Symp. Water Rep. Soils, Riverside, CA. 6–10 May 1968. Univ. of Calif., Riverside.

Brooks, R.H., and A.T. Corey. 1964. Hydraulic properties of porous media. Hydrol. Pap. 3. Colorado State Univ., Fort Collins.

DeBano, L.F. 1969. Observations on water-repellent soils in western United States. p. 17–29. *In* Proc. Symp. Water Rep. Soils, Riverside, CA. 6–10 May 1968. Univ. of Calif., Riverside.

Dekker, L.W. 1988. Verspreiding, oorzaken, gevolgen en verbeterings mogelijkheden van waterafstotende gronden in Nederland. Rep. 2046. Soil Surv. Inst., Wageningen, the Netherlands.

Dekker, L.W., and P.D. Jungerius. 1990. Water repellency in the dunes with special reference to the Netherlands. Catena Suppl. 18:173–183.

Dekker, L.W., and C.J. Ritsema. 1994. How water moves in à water repellent sandy soil. 1. Potential and actual repellency. Water Resour. Res. 30:2507–2517.

Dekker, L.W., and C.J. Ritsema. 1996. Preferential flow paths in a water repellent clay soil with grass cover. Water Resour. Res. 32:1239–1249.

Gilmour, D.A. 1968. Water repellence of soils related to surface dryness. Aust. For. 32:143–148.

Glass, R.J., T.S. Steenhuis, and J.-Y. Parlange. 1989a. Wetting front instability. 2. Experimental determination of relationships between system parameters and two-dimensional unstable flow field behavior in initially dry porous media. Water Resour. Res. 25:1195–1207.

Glass, R.J., T.S. Steenhuis, and J.-Y. Parlange. 1989b. Mechanism for finger persistence in homogeneous, unsaturated, porous media: Theory and verification. Soil Sci. 148:60–70.

Hendrickx, J.M.H., L.W. Dekker, and O.H. Boersma. 1993. Unstable wetting fronts in water-repellent field soils. J. Environ. Qual. 22: 109–118.

Hendrickx, J.M.H., L.W. Dekker, E.J. van Zuilen, and O.H. Boersma. 1988. Water and solute movement through a water repellent sand soil with grasscover. p. 131–146. *In* P.J. Wierenga and D. Bachelet (ed.) Validation of flow and transport models for the unsaturated zone. Proc. Int. Conf. and Worksh., Ruidoso, NM. 23–26 May 1988. New Mexico State Univ., Las Cruces.

Jamison, V.C. 1945. The penetration of irrigation and rain water into sandy soil of central Florida. Soil Sci. Soc. Am. Proc. 10:25–29.

King, P.M. 1981. Comparison of methods for measuring severity of water repellence of sandy soils and assessment of some factors that affect its measurements. Aust. J. Soil Res. 19:275–285.

Letey, J. 1969. Measurement of contact angle, water drop penetration time, and critical surface tensions. p. 43–47. *In* Proc. Symp. Water Rep. Soils, Riverside, CA. 6–10 May 1968. Univ. of Calif., Riverside.

Liu, Y., T.S. Steenhuis, and J.-Y. Parlange. 1994. Closed form solution for finger width in sandy soils at different water contents. Water Resour. Res. 30:949–952.

Marshall, T.J., and J.W. Holmes. 1979. Soil physics. Cambridge Univ. Press, Cambridge, England.

Nakaya, N. 1982. Water repellency of soils. JARQ 16(1):24–28.

Parlange, J.-Y., and D.E. Hill. 1976. Theoretical analysis of wetting front instability in soils. Soil Sci. 122:236–239.

Raats, P.A.C. 1973. Unstable wetting fronts in uniform and nonuniform soils. Soil Sci. Soc. Am. Proc. 37:681–685.

Saffman, P.G., and G. Taylor. 1958. The penetration of a fluid into a porous medium or Hele–Shaw cell containing a more viscous liquid. Proc. R. Soc. London A245:312–331.

Selker, J.S., P. Leclerq, J.-Y. Parlange, and T.S. Steenhuis. 1992a. Fingered flow in two dimensions. 1. Measurement of matric potential. Water Resour. Res. 28:2513–2521.

Selker, J.S., T.S. Steenhuis, and J.-Y. Parlange. 1992b. Fingered flow in two dimensions. 2. Predicting finger moisture profile. Water Resour. Res. 28:2523–2528.

Wallis, M.G., and D.J. Horne. 1992. Soil water repellency. Adv. Soil. Sci. 20:91–146.

Weitz, D.A., J.P. Stokes, R.C. Ball, and A.P. Kushnick. 1987. Dynamic capillary pressure in porous media: Origin of the viscous-fingering length scale. Phys. Rev. Lett. 59:2967–2970.